Supporting Information

Easy Conversion-Perovskite Fluorides $KCo_{1-x}Fe_xF_3$ for Efficient Oxygen Evolution Reaction

Yilei Du‡[a,b], Genyan Hao‡[c], Tao Zhao[a,b], Dandan Li[d], Guang Liu[a,b], Dazhong Zhong[a,b,*], Jinping Li[a,b], Qiang Zhao[a,b,*]

[a] College of Chemical Engineering and Technology, Taiyuan University of Technology, Taiyuan 030024, Shanxi, P.R. China.

[b] Shanxi Key Laboratory of Gas Energy Efficient and Clean Utilization, Taiyuan 030024, Shanxi, P.R. China.

[c] Shanxi College of Technology, Shuozhou 036000, Shanxi, P.R. China.

[d] Shandong Provincial Key Laboratory of Chemical Energy Storage and Novel Cell Technology, School of Chemistry and Chemical Engineering, Liaocheng University, Liaocheng 252059, Shandong, P.R. China.

‡ These two authors contributed equally to this work.

*Corresponding author

zhongdazhong@tyut.edu.cn(D.Z. Zhong);

zhaoqiang@tyut.edu.cn(Q. Zhao).

Experimental section

Materials

Electrocatalyst Synthesis: $KF\cdot 2H_2O$ (AR 99%), $CoCl_2\cdot 6H_2O$ (AR 98.00%), $Co(NO_3)_2\cdot 6H_2O$ (AR 99%), $FeSO_4\cdot 7H_2O$ (AR 99.0%), KOH (AR 85%), ethylene glycol, ethanol, hydrochloric acid (HCl), NF was purchased from The Source of Power Battery Material Co., Ltd. (Shanxi, China). Before synthesis, NF (4 cm × 3 cm) was sonicated with 2 M HCl, ultrapure water, and ethanol under ultrasound for several minutes, respectively.

Preparation of the catalysts

perovskite fluorides synthesis

By a one-step solvothermal process, perovskite fluorides, $KCoF_3$, $KCo_{0.9}Fe_{0.1}F_3$, $KCo_{0.8}Fe_{0.2}F_3$, $KCo_{0.6}Fe_{0.4}F_3$, $KCo_{0.5}Fe_{0.5}F_3$, $KCo_{0.4}Fe_{0.6}F_3$ and $KFeF_3$ were synthesized on NF. As an illustration, consider the preparation of $KCo_{0.5}Fe_{0.5}F_3$@NF as an example. Firstly, 6 mmol $CoCl_2\cdot 6H_2O$, 6 mmol $FeSO_4\cdot 7H_2O$, 36 mmol $KF\cdot 2H_2O$, and 30 mL ethylene glycol were mixed and stirred vigorously until completely dissolved. Subsequently, the above uniform solution and the blank NF was transferred into a 50 mL Teflon vessel, followed by heating to 180 °C for 20 hours to generate the $KCo_{0.5}Fe_{0.5}F_3$@NF electrocatalyst. After the above operations, NF was washed with ethylene glycol and ultrapure water, and finally dried at 100 °C over the night to produce the $KCo_{0.5}Fe_{0.5}F_3$@NF. The other samples that the total molar amount of metal ions remains unchanged, the dosage of $CoCl_2\cdot 6H_2O$ and $FeSO_4\cdot 7H_2O$ were adjusted according to the ratio of Co:Fe, and other operations were the same as above.

$CoFeO_x$@NF synthesis

Co-Fe LDH@NF was prepared by electrodeposition with NF as the substrate in a mixed solution of $Co(NO_3)_2\cdot 6H_2O$ (0.5 mM), $Fe(NO_3)_3\cdot 9H_2O$ (0.5 mM) at -1 V (vs. Ag/AgCl) electrodeposition for 1800 s at room temperature (electrode area: 2 cm^2), then dried at 60 °C in an oven all night long. The prepared Co-Fe LDH@NF was transferred to a tube furnace and held in the air at a heating rate of 5 °C/min to 500 °C for 2 hours to obtain the $CoFeO_x$@NF.

Characterization

The phase analysis of the catalysts was analyzed by scanning electron microscope (SEM), energy-dispersive X-ray spectrometry (EDS) (Hitachi, SU8010, Tokyo, Japan), and a transmission electron microscope (TEM) (Japan). X-ray diffraction (XRD) was acquired on a D8 Bruker with Cu-Ka radiation (k = 1.5418 Å). X-ray photoelectron spectroscopy (XPS) was performed with an ESCALAB 220i-XL spectrometer (VG Scientific, UK) with Al-Kα radiation (h = 1486.6 eV, 150 W). Inductively coupled plasma optical emission spectrometer (ICP-OES) measurements were performed using an avio^{TM} 200 ICP-OES (TJA, Franklin, USA).

Electrochemical measurements

A Princeton electrochemical workstation (PARSTATMC, Princeton, USA) was used to control a standard three-electrode system in order to measure the electrochemical performance. Electrocatalysts based on NF, Pt rod and Hg/HgO were used as the working electrode, counter electrode and reference electrode, respectively., Linear sweep voltammetry (LSV) was collected at a sweep speed of 2 mV s^{-1} from 1 V (vs. Hg/HgO) to 0 V in 1.0 M KOH. The Electrochemical Impedance Spectroscopy (EIS) curve was performed at 0.6 V (vs. Hg/HgO) in the frequency range of 10^5 Hz to 0.05 Hz in 1.0 M KOH. Double-layer capacitance (C_{dl}) was used to define the electrochemically active surface area (ECSA), and Tafel slope was found by fitting an LSV curve. Using the formula $E_{RHE} = E_{Hg/HgO} + 0.098 + 0.059*pH - iR$, all electrochemical data have been calibrated and translated to the reversible hydrogen electrode (RHE). The formula for calculating overpotential (η) is $\eta = E_{RHE} - 1.23$ V. The Tafel slope was obtained according to the formula: $E_{RHE} = a + b*\log j$. Faradaic efficiency calculation formula: $FE = [4(V/V_{25℃}) *N_A * 1.6 * 10^{-19}]/Q$.

In-situ Raman spectroscopy test

This test was conducted in a custom-built electrochemical cell. In order to minimize the effect of bubbles generated during the OER process on spectral collection, the electrolyte was replaced with 0.1 M KOH. Other than this, the

conditions were consistent with the electrochemical performance tests. In the potential range of 1.05 to 1.65 V (vs. RHE), a constant voltage was applied at 0.1 V intervals for 3 min, and then in-situ Raman spectra of the laser intensity of 532 nm were collected.

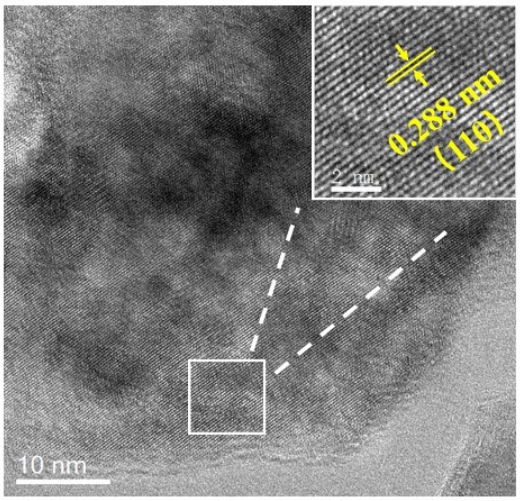

Fig. S1 TEM image of $KCo_{0.5}Fe_{0.5}F_3$@NF.

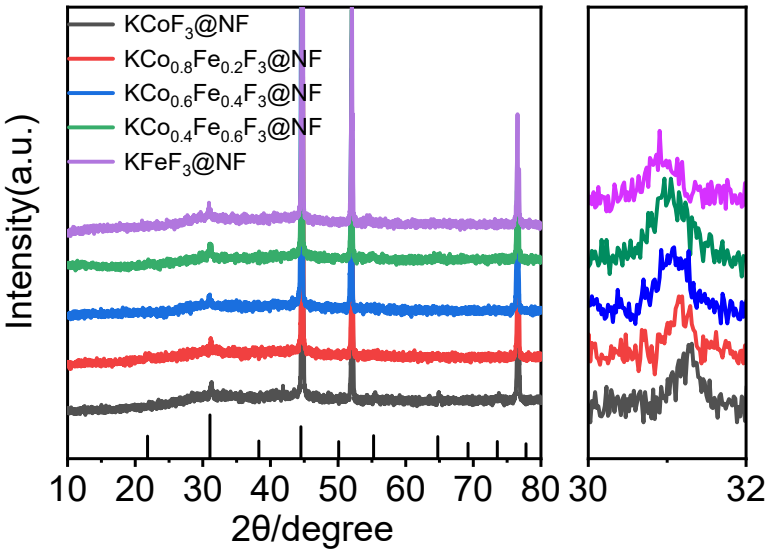

Fig. S2. XRD patterns of $KCoF_3$@NF, $KCo_{0.8}Fe_{0.2}F_3$@NF, $KCo_{0.6}Fe_{0.4}F_3$@NF, $KCo_{0.4}Fe_{0.6}F_3$@NF and $KFeF_3$@NF.

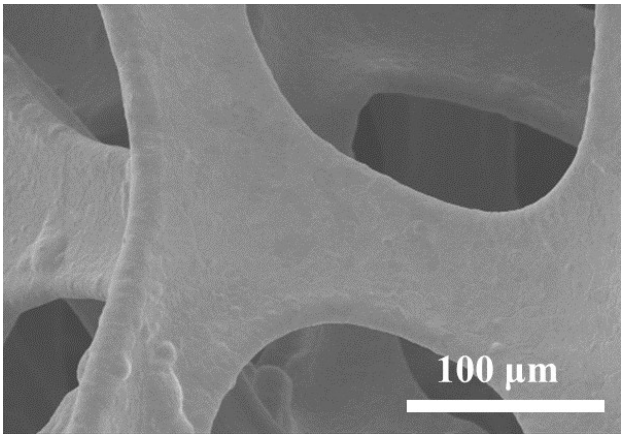

Fig. S3. SEM image of Pure NF.

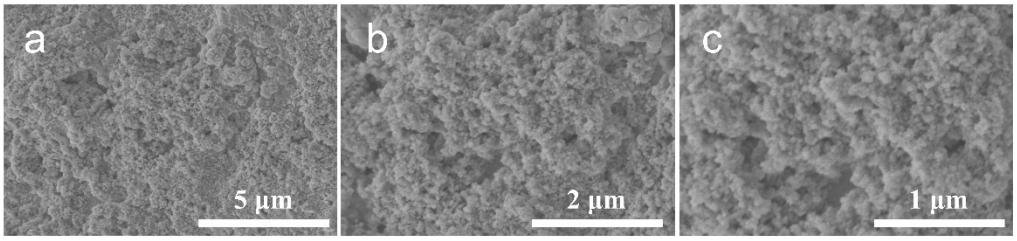

Fig. S4. SEM image of $KCo_{0.5}Fe_{0.5}F_3$@NF.

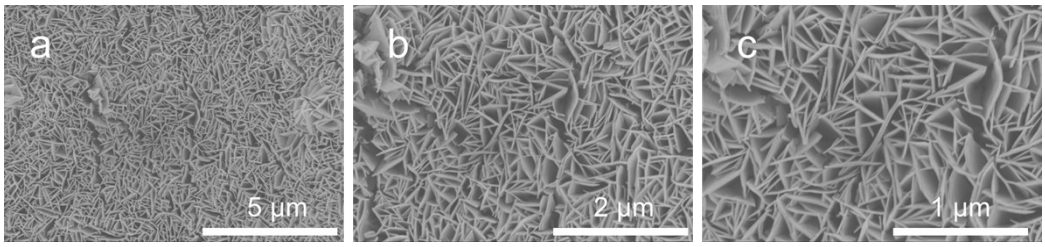

Fig. S5. SEM image of $CoFeO_x$@NF.

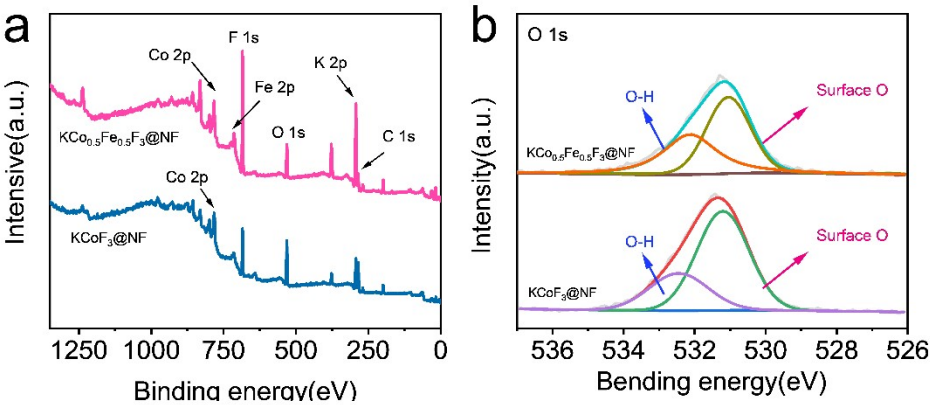

Fig. S6. XPS spectra of (a) Full XPS pattern, (b) O 1s of $KCoF_3$@NF and $KCo_{0.5}Fe_{0.5}F_3$@NF.

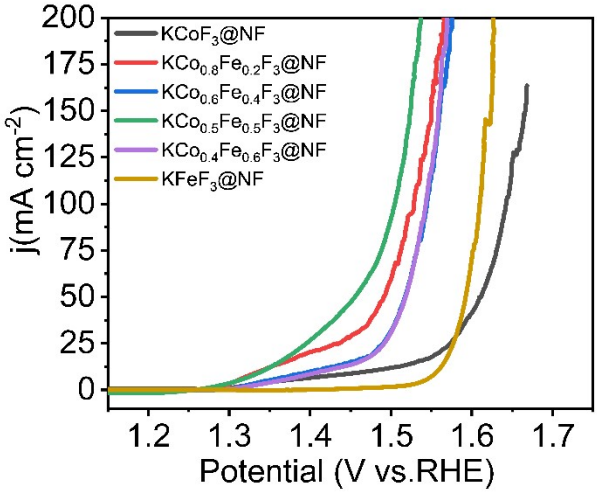

Fig. S7. The polarization curves for $KCoF_3$@NF, $KCo_{0.8}Fe_{0.2}F_3$@NF, $KCo_{0.6}Fe_{0.4}F_3$@NF, $KCo_{0.5}Fe_{0.5}F_3$@NF, $KCo_{0.4}Fe_{0.6}F_3$@NF and $KFeF_3$@NF.

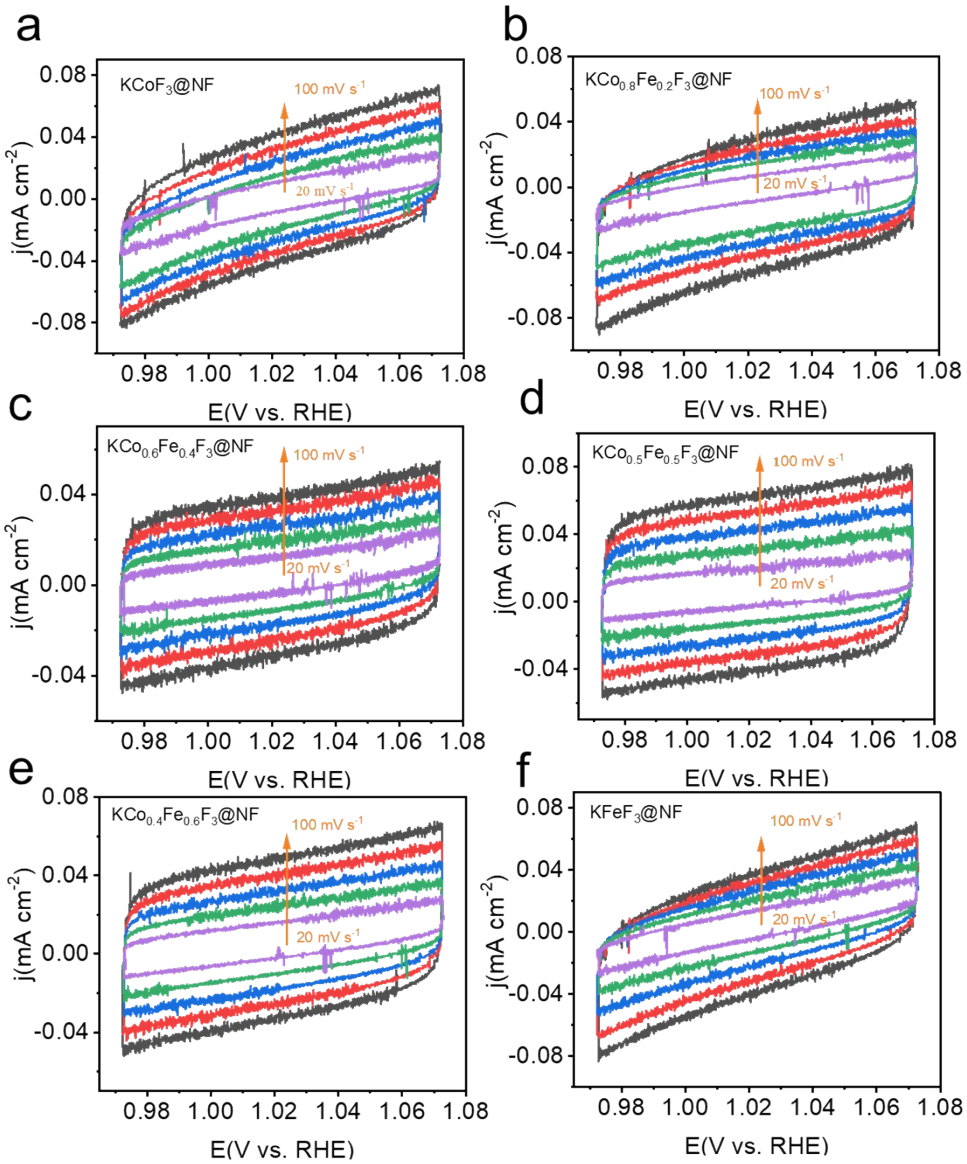

Fig. S8. CV curves at various scan rates in the potential range of 0.97 – 1.07 V vs RHE for (a) $KCoF_3$@NF, (b) $KCo_{0.8}Fe_{0.2}F_3$@NF, (c) $KCo_{0.6}Fe_{0.4}F_3$@NF, (d) $KCo_{0.5}Fe_{0.5}F_3$@NF, (e) $KCo_{0.4}Fe_{0.6}F_3$@NF and (f) $KFeF_3$@NF.

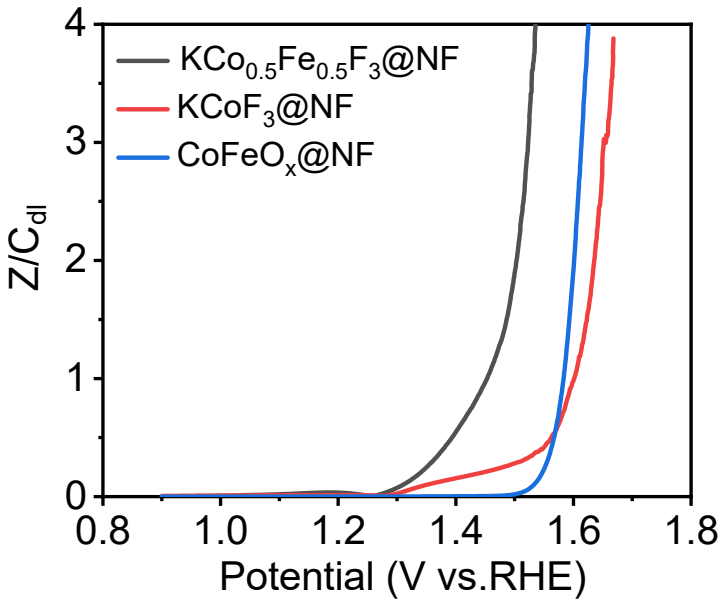

Fig. S9 LSV curve based on ECSA normalization.

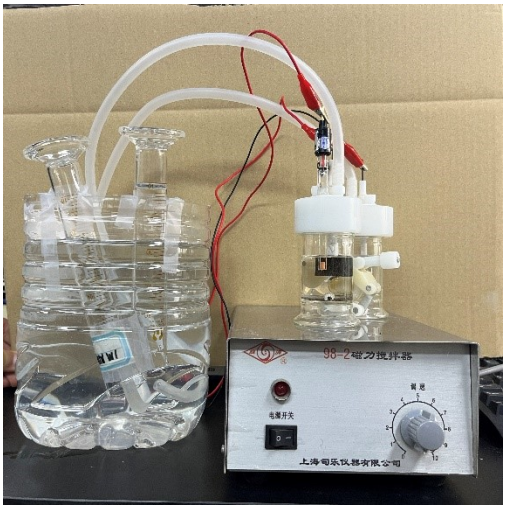

Fig. S10 Drainage device diagram.

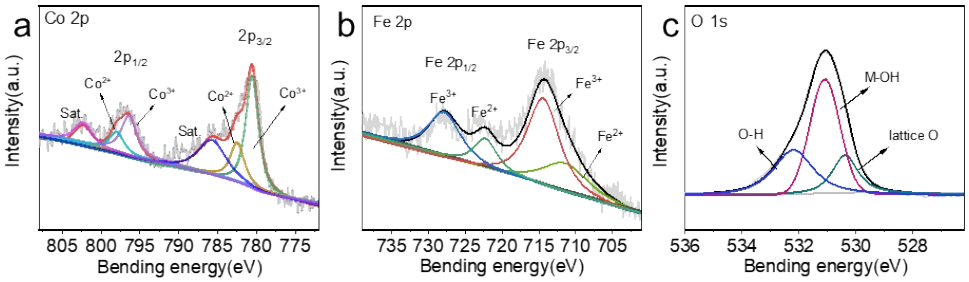

Fig. S11. XPS spectra of (a) Co 2p, (b) Fe 2p (c) O 1s of $KCo_{0.5}Fe_{0.5}O_3$@NF electrocatalyst after OER.

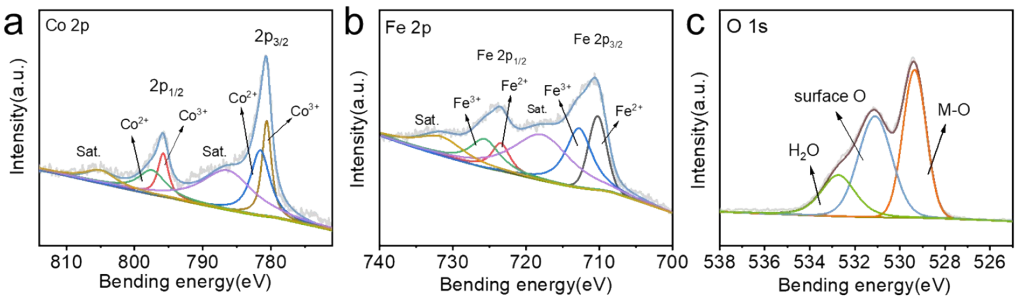

Fig. S12. XPS spectra of (a) Co 2p, (b) Fe 2p (c) O 1s of $CoFeO_x$@NF electrocatalyst after OER.

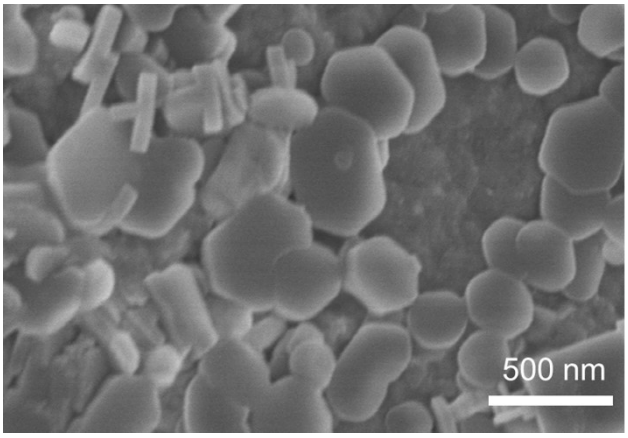

Fig. S13. SEM image of $KCo_{0.5}Fe_{0.5}F_3$@NF electrocatalyst after OER.

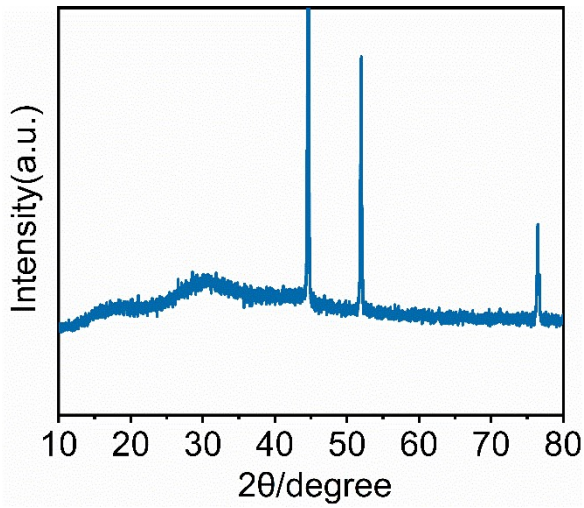

Fig. S14. XRD patterns of $KCo_{0.5}Fe_{0.5}F_3$@NF electrocatalyst after OER.

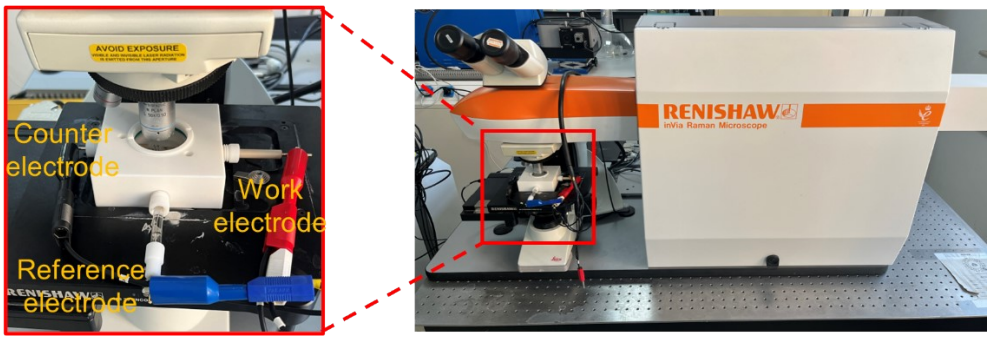

Fig. S15 Custom-built electrochemical cell for in-situ Raman spectra collection.

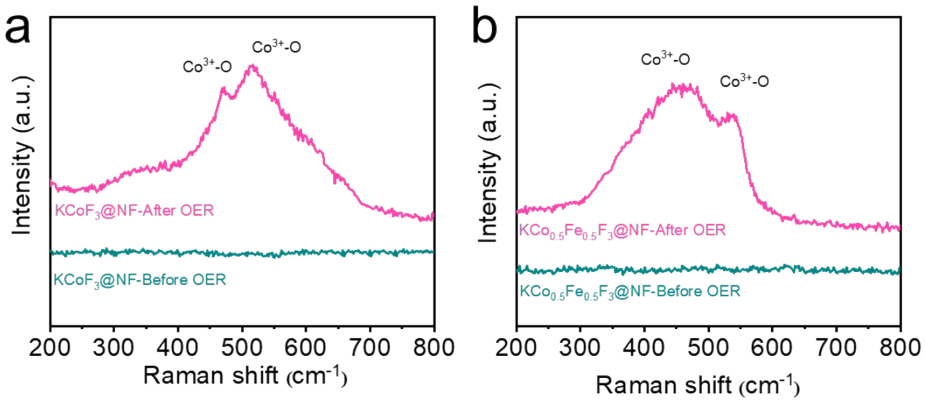

Fig. S16. Ex-situ Raman spectra of (a) $KCoF_3$@NF and (b) $KCo_{0.5}Fe_{0.5}F_3$@NF electrocatalysts before and after OER.

Table S1. Atomic concentration of Co:Fe in perovskite fluorides determined via ICP-OES.

samples	Co (Atomic ratio)	Fe (Atomic ratio)
$KCo_{0.8}Fe_{0.2}F_3$@NF	79.36	21.64
$KCo_{0.6}Fe_{0.4}F_3$@NF	62.17	37.83
$KCo_{0.5}Fe_{0.5}F_3$@NF	52.84	47.16
$KCo_{0.4}Fe_{0.6}F_3$@NF	41.35	58.65

Table S2. Atomic concentration of $KCo_{0.5}Fe_{0.5}F_3$@NF obtained by XPS.

	Atomic (%)
F	44.54
Co	10.2
Fe	9.38
O	16.7

Table S3. Atomic concentration of $KCo_{0.5}Fe_{0.5}F_3$@NF-After OER obtained by XPS.

	Atomic (%)
F	10.99
Co	4.42
Fe	3.61
O	41.87

Table S4. Comparison of the overpotentials for $KCo_{0.5}Fe_{0.5}F_3$@NF and the previously reported OER catalysts.

Catalysts	electrolyte	Overpotential [mV]@ Current density [mA cm^{-2}]	Ref.
$KCo_{0.5}Fe_{0.5}F_3$@NF	1.0 M KOH	118@10 150@20	This work
$La_{0.7}Sr_{0.3}CoO_{3-\delta}$	1.0 M KOH	326@10	[1]
$Sr_{0.9}Fe_{0.6}Co_{0.2}Ni_{0.2}O_{3-\delta}$	1.0 M KOH	340@10	[2]
$La_{1.8}CoMnO_{6-\delta}$	1.0 M KOH	350@10	[3]
$LaCo_{0.8}V_{0.2}O_3$	1.0 M KOH	306@10	[4]
$LaCo_{0.75}Fe_{0.25}O_3$	1.0 M KOH	310@10	[5]
$Sr_{0.95}Ce_{0.05}Fe_{0.9}Ni_{0.1}O_{3-\delta}$	1.0 M KOH	340@10	[6]
$La_{0.6}Sr_{0.4}Co_{0.8}Fe_{0.2}O_3$	1.0 M KOH	353@10	[7]
$Pr_{0.5}Ba_{0.5}Fe_{0.975}Ni_{0.025}O_{3-\delta}$	0.1 M KOH	440@10	[8]
$La_{0.6}Sr_{0.4}Co_{0.8}Ni_{0.2}O_{3-\delta}$	1.0 M KOH	320@10	[9]
$SrCo_{0.95}Si_{0.05}O_{3-\delta}$	1.0 M KOH	410@10	[10]
$PrBa_{0.5}Sr_{0.5}Co_{1.5}Fe_{0.5}O_{4.7+\delta}Cl_{0.3}$	1.0 M KOH	330@10	[11]
$La_{0.8}Sr_{1.2}Co_{0.2}Fe_{0.8}O_{4+\delta}$	1.0 M KOH	350@10	[12]
F-$Ba_{0.5}Sr_{0.5}Co_{0.8}Fe_{0.2}O_{3-\delta}$	1.0 M KOH	280@10	[13]
$Pr_{0.5}Sr_{0.5}Co_{0.8}Fe_{0.2}O_{3-\delta}$	1.0 M KOH	320@10	[14]
$Ba_{0.9}Sr_{0.1}Co_{0.8}Fe_{0.2}O_{3-\delta}$	1.0 M KOH	300@10	[15]

Reference：

[1] Y. Lu, A. Ma, Y. Yu, R. Tan, C. Liu and P. Zhang. *ACS Sustain. Chem. Eng*., 2019, **7**, 2906-2910.

[2] B. Dongyang, W. Yang, Q. Ye, Z. Ma, S. Lai and F. Dong. *J. Alloys Compd*., 2023, **958**, 170368.

[3] S.-F. Li, J. Zheng and D. Yan. *Inorg Chem*., 2023, **62**, 11009-11015.

[4] Y. Sun, Z. Zhao, S. Wu, W. Li, B. Wu and G. Liu. *ChemSusChem*., 2020, **13**, 2671-6.

[5] B. Bao, Y. Liu, M. Sun, B. Huan, Y. Hu and P. Da. *Small*., 2022, **18**, 2201131.

[6] S. She, Y. Zhu, X. Wu, Z. Hu, A. Shelke and W.-F. Pong. *Adv. Funct. Mater*., 2022, **32**, 2111091.

[7] L. Zhang, H. Zhu, J. Hao, C. Wang, Y. Wen and H. Li. *Electrochim. Acta*., 2019, **327**, 135033.

[8] L. Gui, Z. Huang, G. Li, Q. Wang, B. He and L. Zhao. *Electrochim. Acta*., 2019, **293**, 240-246.

[9] Y. Niu, X. Chang, M. Zhang and J. Mu. *Ceram. Int*., 2024, **5**, 137-146.

[10] Y. Wang, G. Chen, J. Xie and D. *Int. J. Hydrogen Energy*., 2022, **47**, 39108-39119.

[11] T. Wang, Y. Wang, Y. Zhao and Y. Bu. *Energy & Fuels*., 2023, **38**, 671-681.

[12] C. Li, Y. Wang, C. Jin, J. Lu, J. Sun and R. Yang. *Int. J. Hydrogen Energy*. 2020, **45**, 22959-22964.

[13] J. Xiong, H. Zhong, J. Li, X. Zhang, J. Shi and W. Cai. *Appl. Catal. B-Environ*., 2019, **256**, 117817.

[14] S. Wu, J. Li, J. Hu, Y. Huang, H.-S. Xu, K. Tang. *ACS Appl. Energy Mater*., 2023, **6**, 6289-6298.

[15] Q. Luo, D. Lin, W. Zhan, W. Zhang, L. Tang, J. Luo. *ACS Appl. Energy Mater*. 2020, **3**, 7149-7158.